Experimental and theoretical study of the efficiency of a three-electrode reactor for the removal of NO

2014 J. Phys. D: Appl. Phys. 47 205202

(http://iopscience.iop.org/0022-3727/47/20/205202)

IOP Publishing Journal of Physics D: Applied Physics
J. Phys. D: Appl. Phys. **47** (2014) 205202 (9pp) doi:10.1088/0022-3727/47/20/205202

Experimental and theoretical study of the efficiency of a three-electrode reactor for the removal of NO

J L Gallego[1], F Minotti[2] and D Grondona[2]

Instituto de Física del Plasma (INFIP), Consejo Nacional de Investigaciones Científicas y Técnicas (CONICET)-Departamento de Física, Facultad de Ciencias Exactas y Naturales, Universidad de Buenos Aires (UBA), C1428EHA, Buenos Aires, Argentina

E-mail: grondana@df.uba.ar

Received 17 February 2014, revised 19 March 2014
Accepted for publication 27 March 2014
Published 1 May 2014

Abstract

An experimental and theoretical study is presented on the efficiency of the removal of NO in a N_2 atmosphere in a novel three-electrode reactor. This reactor combines a dielectric-barrier discharge with a corona discharge, designed to enhance streamer propagation in a relatively large region. Experimentally, the reactor has a good energy yield for the removal of NO, as compared with other discharge methods. A theoretical model is developed for the production of reactive species in the streamers by different reactions that allow to relate simple electrical measurements with the reactor efficiency. This theoretical efficiency resulted in good agreement with the experimental one, validating the model and allowing the evaluation of the contribution of different reactions involved in NO removal.

Keywords: nonthermal plasma, NO removal, electric discharge

(Some figures may appear in colour only in the online journal)

List of variables employed

a	radius of the external electrode
a_d	radius of the disc electrode
A_s	local cross section of the streamer channel
ΔV	voltage difference in gap crossed by the streamers
ΔV_{L_s}	voltage difference along a streamer channel length L_s
ε_0	permittivity of the vacuum
ε_r	relative permittivity of the dielectric
ε_p	reactor efficiency for the destruction of molecules p
ε_p^c	contribution of the streamer channel to the efficiency ε_p
ε_p^h	contribution of the streamer heads to the efficiency ε_p
ε_{exp}	experimental efficiency for the destruction of NO
$\varepsilon_{exp}\%$	percental experimental efficiency for the destruction of NO
E	electric field component along the streamer channel
E_h	electric field of the streamer head (radial component)
$E_{h\,max}$	maximum value of the electric field of the streamer head
E_L	component of the Laplacian electric field along the streamer channel
E_c	energy cost per removed NO molecule
E_y	energy yield for the removal of NO (number of mol of removed NO per unit energy input)
G_q	G-value for reaction q
G_{eff}^q	effective G-value for reaction q
I	current between active disc electrode and external electrode (interelectrode current)
I_{DBD}	current between disc electrodes (DBD current)
i_s	current in a streamer
I_{st}	total current including all present streamers
k_q	rate coefficient for reaction q
k_{pq}	rate coefficient of reaction with intervening molecules q destroying molecules p

[1] Fellow of CONICET.
[2] Researcher of CONICET.

L_s length of the streamer channel
n_0 total number density (including all present molecules)
n_e number density of electrons
n_m number density of gas molecules intervening in a reaction
n_m^q number density of molecules m intervening in reaction q
n_p number density of molecules p destroyed in a reaction
n_q number density of molecules produced in reaction q
N_p total number of molecules p
N_q total number of molecules q
N_{st} total number of streamers
q_d electric charge on the disc electrode
Q volumetric flow rate through the reactor
r_h radius of the streamer head
v_D drift velocity of electrons
V_{ac} voltage of the ac power supply
V_{ac}^p peak-to-peak value of V_{ac}
V_{dc} voltage of the dc power supply
V_{ch} volume of reactor chamber
z_d axial position of the disc electrode

1. Introduction

The study of non-thermal plasma for the removal of pollutants like NO is a subject of interest for industrial applications and fundamental academic studies. The plasma is generated with an electrical discharge at atmospheric pressure. Without heating of the gas, the electrical energy goes into the production of energetic electrons, which collide with gas molecules and produce a rich variety of chemical products that undergo reactions capable of transforming harmful substances into non-hazardous products.

There are many studies of NO degradation, using different discharge configurations, which employ plasma technologies with good results. Some of them are pulsed positive and negative corona discharges (CDs) [1, 2], dielectric barrier discharges (DBDs) [3–6] and plasma–catalyst hybrid systems [7–9]. Most of all reactor configurations studied consist of small setups with a small plasma volume or with a high resistance to the gas flow, like the DBD packed bed configuration.

In previous work [10] the development of a three-electrode discharge with cylindrical geometry, which could be long-time sustained over interelectrode air gaps up to 20–25 mm, was presented. The discharge was based on the combination of a DBD with a CD in a three-electrode system, and essentially resulted from the 'stretching' of streamers of the DBD by the action of a CD generated between the active electrode of the DBD and a remote third electrode. This discharge configuration presents a large plasma volume and a natural boundary for the gas flow.

In this work the efficiency of NO removal in a N_2 atmosphere, employing a cylindrical three-electrode discharge configuration, is studied both experimentally and theoretically. In the theoretical study we have developed a 'microscopic model' based on the assumption that the reacting species are generated mainly by electron processes in the streamers [11, 12]. The required information of the streamer characteristics needed for the model is obtained from instantaneous current measurements. Besides, as the efficiency depends strongly on the G-value [13] for the electron process considered, which is in turn a function strongly dependent on the reduced electric field, a difficult problem arises, because the electric field in the streamer channel and head are very different in magnitude and spatial extension. Using the Bolsig software [14] the G-values of interest are obtained as functions of the reduced electric field. The electric field in the streamer channels is obtained analytically from the electrodes geometry and applied voltages, while a simple model of a spherical head is used to estimate the contribution from the electric field in the streamer head. As was previously determined theoretically by Naidis [12] and experimentally by Kozlov [15], it is found also here that the streamer heads are more important than the streamer channels for the production of reactive species, at least for reactions with relatively high energy thresholds as those involved in this work. The novelty of the present approach lies in that sensitive parameters determining the reactor efficiency, like streamer channel radius, time-resolved number of streamers, streamer head characteristics, etc, are finally not needed since their effect ends up being included in easily measurable discharge parameters.

2. Experimental setup

A schematic of the experimental setup is shown in figure 1. The reactor has an electrode system consisting in two discs of adhesive aluminum tape of 50 μm of thickness and 34 and 38 mm of diameters, flush mounted at both sides of a poly-methyl methacrylate dielectric disc of 40 mm diameter and 2 mm width. One of the discs (electrode 1) is connected to an ac power supply and the other (electrode 2) to ground by wires placed inside two insulating tubes (10 mm in diameter) which pass along the electrode system. A third electrode, consisting in a steel mesh (electrode 3) connected to a dc power supply is attached to the inner wall of a poly-methyl methacrylate dielectric cylindrical tube with 80 mm inner diameter, 240 mm length and with a wall thickness of 5 mm. This tube surrounds the central electrode arrangement and the distance between the edges of the central electrodes and the third electrode is 20 mm. Two plates seal the ends of the tube. The gas, under pressure, goes through the reactor. The gas inlet is placed at one plate and the gas outlet in the other plate.

The dc power supply (V_{dc}) output is a continuous negative voltage variable in the range -9 to -20 kV. The ac power supply (V_{ac}) consists in a function generator coupled to an audio-amplifier (power of 700 W) that feeds a high voltage transformer. In practice, there is an optimal matching frequency, corresponding to the resonance between the transformer inductance and the stray capacity of the electrode arrangement, including the wire connections.

The development of the discharge requires the presence of a positive cycle of a well developed DBD together with a

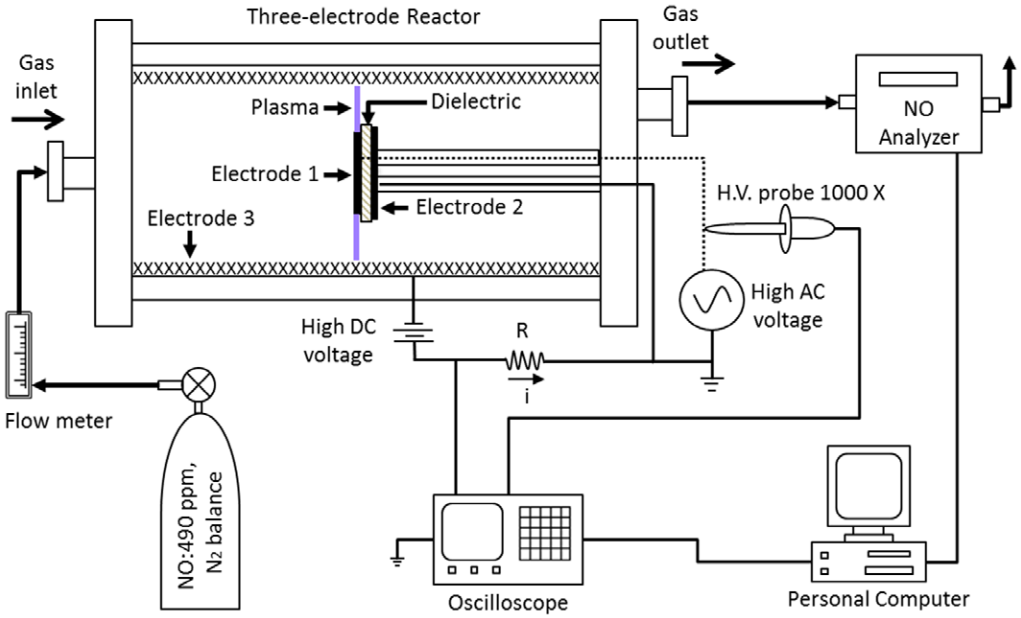

Figure 1. Experimental setup.

CD at the third electrode, the mesh, performing as the cathode; and a voltage drop between the DBD electrode and the mesh high enough to obtain an average electric field in the gap that must exceed a minimum average electric field value necessary for the streamer propagation across the gap.

The discharge is composed of a train of streamers which cross the gap with an average velocity of $(1.2 \pm 0.2)\, 10^5\, \mathrm{m\, s^{-1}}$ [10], so it takes each separate streamer about 150 ns to cross the interelectrode space.

For our circuit, the optimum excitation ac frequency was $f_{\mathrm{ac}} = 5.3\,\mathrm{kHz}$. The ac peak-to-peak voltage ($V_{\mathrm{ac}}^{\mathrm{p}}$) range is 0–30 kV. The voltage was measured using a high voltage probe ($1000 \times /3.0\,\mathrm{pF}/100\,\mathrm{M\Omega}$). Current measurements were inferred from the voltage drop through a 50 Ω resistance. These electrical signals were registered with a four-channel digitizing oscilloscope with a bandwidth of 60 MHz and $1\,\mathrm{Gs\, s^{-1}}$ of sampling rate.

The operating gas was NO 490 ppm, N_2 balanced. The gas flow Q, measured using a flow meter, was $1.5\,\mathrm{l\,min^{-1}}$. The inlet and outlet concentrations of NO were measured by a gas analyser MaMos 300 with an uncertainty of 1%.

3. Theoretical model of the reactor efficiency

In order to model the efficiency of the device we will consider that the largest part of the dissociation, excitation and ionization of the gas molecules by electron impact, takes place in the streamers [11, 12] which cross the electrode gap and reach the external electrode.

We will separately analyse the contributions from the streamer channel and from the streamer head, as both regions of the streamer have quite different electric field magnitudes.

Streamer channel contribution. We proceed by considering first the streamer channel contribution to the efficiency. For this, we take a generic reaction that generates molecules of species q due to electron impact, represented by

$$\frac{\mathrm{d}n_q}{\mathrm{d}t} = k_q n_{\mathrm{e}} n_m, \tag{1}$$

where n_q is the number density of q molecules, n_{e} and n_m the local number densities of electrons and of gas molecules intervening in the reaction, respectively, and k_q is the rate coefficient. In this way, the number of reactions per unit time is given by the volume integral of equation (1), extended to the volume comprised by the channels of all the streamers present,

$$\left.\frac{\mathrm{d}N_q}{\mathrm{d}t}\right)_s = \sum_{s=1}^{N_{\mathrm{st}}} \int_0^{L_{\mathrm{s}}} k_q n_{\mathrm{e}} n_m A_{\mathrm{s}}(x)\, \mathrm{d}x, \tag{2}$$

where the summation is extended to the N_{st} streamers present at the time considered, and the line integral comprises the length L_{s} of each streamer, of local cross section area $A_{\mathrm{s}}(x)$.

A convenient recasting of equation (2) can be done using the G value [13], that is, the number of reactions per 100 eV of input energy, which in SI units is given by (the factor 100 has units of volt)

$$G_q = \frac{k_q n_0}{E\, v_D} \times 100, \tag{3}$$

where n_0 is the total gas number density, v_{D} is the electron drift velocity and E is the electric field strength in the streamer channel. This allows to write equation (2) as

$$\left.\frac{\mathrm{d}N_q}{\mathrm{d}t}\right)_s = \frac{1}{100} \sum_{s=1}^{N_{\mathrm{st}}} \int_0^{L_{\mathrm{s}}} \frac{G_q E}{n_0} v_{\mathrm{D}} n_{\mathrm{e}} n_m A_{\mathrm{s}}(x)\, \mathrm{d}x. \tag{4}$$

On the other hand, the instantaneous electric current due to the electrons and ions in a single streamer channel can be expressed as [16]

$$i_{\mathrm{s}} = \frac{e}{\Delta V_{L_{\mathrm{s}}}} \int_0^{L_{\mathrm{s}}} (n_{\mathrm{e}} v_{\mathrm{D}} + n_{\mathrm{i}} v_{\mathrm{i}})\, A_{\mathrm{s}}(x) E_{\mathrm{L}}\, \mathrm{d}x, \tag{5}$$

where the absolute value of all magnitudes has been taken, e is the value of the elementary charge, and E_L is the applied Laplacian electric field, with corresponding potential difference ΔV_{L_s} along the streamer length. Neglecting the ion drift velocity v_i, as compared to that of the electrons, it is seen that the integrand in expression (5) includes many of the factors in the integrand in (4). In fact, as in the streamer channel the electric field is practically equal to the applied field [17], one can write $E_L = E$, and so, also assuming uniform densities of the total gas n_0, and of the reacting molecules n_m, and replacing G_q by an effective, constant value G^q_{eff} (to be determined latter), we can write (4) as

$$\left.\frac{dN_q}{dt}\right)_s = \frac{G^q_{\text{eff}}}{100}\frac{n_m}{n_0 e}\sum_{s=1}^{N_{st}} \Delta V_{L_s} i_s. \tag{6}$$

As only the streamers that cross the entire gap are considered, they all have the same ΔV_{L_s}, the absolute value of the interelectrode potential difference: ΔV, so that

$$\left.\frac{dN_q}{dt}\right)_s = \frac{G^q_{\text{eff}}}{100}\frac{n_m}{n_0 e} I_{st}\Delta V, \tag{7}$$

where I_{st} is the instantaneous electric current due to all the streamers present, which can be determined directly from the electrical measurements.

Consider now that the species q generated in the reaction (1) destroys the species p, through the reaction

$$\frac{dn_p}{dt} = -k_{pq} n_p n_q, \tag{8}$$

so that, assuming uniform concentration of species p, the integration of (8) in the volume of the reactor indicates that the number of destroyed molecules of species p (and also of species q) in the time unit is

$$\frac{dN_p}{dt} = k_{pq} n_p N_q. \tag{9}$$

In this way, the number of q molecules in the reactor is given by the equation (the fraction of q molecules leaving the reactor chamber can be neglected for the usual condition $k_{pq} n_p \gg Q/V_{ch}$, V_{ch} being the chamber reactor volume, and Q the volumetric flow rate through the reactor)

$$\frac{dN_q}{dt} = \left.\frac{dN_q}{dt}\right)_s - k_{pq} n_p N_q. \tag{10}$$

On the other hand, the efficiency for the destruction of p, can be defined as the ratio of the average number of p molecules destroyed per unit time, to the number of p molecules entering the device in the same time unit:

$$\varepsilon_p = \frac{\langle dN_p/dt\rangle}{Q n_p}, \tag{11}$$

where the brackets denote a time average. Using expressions (7), (9), and (10) for the stationary regime ($dN_q/dt = 0$) in equation (11) the contribution from the streamers channels ε^c_p to the reactor efficiency can be expressed as

$$\varepsilon^c_p = \frac{n_m \langle G^q_{\text{eff}} I_{st}\Delta V\rangle}{100 e Q n_0 n_p}. \tag{12}$$

Finally, to specify G^q_{eff} we must consider that G_q is in general a function of the electric field (actually, of the reduced field) [13], so that, formally, G^q_{eff} is, by definition,

$$G^q_{\text{eff}} \equiv \frac{\int_0^{L_s} G_q(E) E n_e v_D A(x)\, dx}{\int_0^{L_s} E n_e v_D A(x)\, dx}. \tag{13}$$

If one considers the evaluation of (13) for the case of a stationary streamer channel, for which electron number conservation implies $n_e v_D A(x) = \text{const}$, the effective G value is evaluated as

$$G^q_{\text{eff}} = \frac{\int_0^{L_s} G_q(E) E\, dx}{\int_0^{L_s} E\, dx} = \frac{\int_0^{L_s} G_q(E) E\, dx}{\Delta V}, \tag{14}$$

and (12) is finally written as

$$\varepsilon^c_p = \frac{n_m \left\langle I_{st}\int_0^{L_s} G_q(E) E\, dx\right\rangle}{100 e Q n_0 n_p}. \tag{15}$$

In the case that multiple reactions of the type represented by equation (1) generate different species q that lead to the destruction of molecules of species p by reactions of the type in equation (8), the number of molecules of species p destroyed in a time unit is given by the generalization of equation (9)

$$\frac{dN_p}{dt} = \sum_q k_{pq} n_p N_q, \tag{16}$$

while the number of molecules of species q is still determined by equation (10), and so the direct generalization of equation (15), obtained for the stationary regime ($dN_q/dt = 0$), is

$$\varepsilon^c_p = \frac{\left\langle I_{st}\sum_q n^q_m \int_0^{L_s} G_q(E) E\, dx\right\rangle}{100 e Q n_0 n_p}, \tag{17}$$

where we have generalized the reaction (1) to allow for the species m to be different for each q, and so have added the upper index q to denote the molecules reacting with the electrons in equation (1) to generate species q.

Note that the time average in equations (15) and (17) can be explicitly done as to each instantaneous value of I_{st} corresponds a measured value ΔV, which in turn, given the electrode geometry, determines the instantaneous electric field distribution needed in relation (14).

Streamer head contribution. To estimate the streamer head contribution we can start with the generic expression (4), where now the electric field is that generated by the streamer head alone, assumed a sphere of radius r_h, so that the spatial coordinate is taken as the distance r to the streamer head centre,

$$\left.\frac{dN_q}{dt}\right)_s = \frac{1}{100}\sum_{s=1}^{N_{st}} \int_{r_h}^{\infty} \frac{G_q E_h}{n_0} v_D n_e n_m A_s(r)\, dr. \tag{18}$$

The integral is formally extended to infinity since the electric field decays rapidly as the inverse of the square of r

$$E_{\mathrm{h}} = E_{\mathrm{h\,max}} \frac{r_{\mathrm{h}}^2}{r^2}, \tag{19}$$

where $E_{\mathrm{h\,max}}$ is the maximum electric field of the streamer head.

We further assume that all streamer heads have the same characteristics so that the field distribution in all them can be considered equal, and taking $v_{\mathrm{D}} n_{\mathrm{e}} A_{\mathrm{s}}(r) \approx i_{\mathrm{s}}/e$ we obtain, as in the case of the streamer channels,

$$\left.\frac{\mathrm{d}N_q}{\mathrm{d}t}\right)_s = \frac{I_{\mathrm{st}}}{100}\frac{n_m}{n_0}\int_{r_{\mathrm{h}}}^{\infty} G_q\,(E_{\mathrm{h}})\,E_{\mathrm{h}}\,\mathrm{d}r, \tag{20}$$

in which the integral can be explicitly done using expression (19) for the electric field. Using (20) the contribution to the efficiency by the streamer heads can be estimated as was done to derive expression (17) resulting in

$$\varepsilon_p^{\mathrm{h}} = \frac{\langle I_{\mathrm{st}}\rangle \sum_q n_m^q \int_{r_{\mathrm{h}}}^{\infty} G_q\,(E_{\mathrm{h}})\,E_{\mathrm{h}}\,\mathrm{d}r}{100 e Q n_0 n_p}, \tag{21}$$

which can be evaluated from the measured current, with the head radius r_{h} and the maximum electric field value $E_{\mathrm{h\,max}}$ as parameters of the model. Alternatively, as the ratio n_m^q/n_0 has generally a known value, proportional to the number of resultant species per unit of intervening molecules, the sum in expression (21) has a unique value depending only on the streamer head parameters, so that it can be determined from a single measurement of the efficiency.

4. Application to the three-electrode reactor

For the case of the particular experiment studied in this work, the reaction of interest in the streamer channels is the generation of atomic nitrogen N by electron impact dissociation of molecular nitrogen N_2, (type of reaction given by equation (1))

$$\mathrm{e} + N_2 \rightarrow \mathrm{e} + \mathrm{N} + \mathrm{N}, \tag{R22}$$

leading to the removal of NO by the reaction (type of reaction given by equation (8))

$$\mathrm{N} + \mathrm{NO} \rightarrow \mathrm{N_2} + \mathrm{O}. \tag{R23}$$

We thus have, corresponding to equation (1),

$$\frac{\mathrm{d}n_{\mathrm{N}}}{\mathrm{d}t} = 2k_{\mathrm{dissoc}} n_{\mathrm{e}} n_{\mathrm{N_2}}, \tag{24}$$

where k_{dissoc} is the rate coefficient for electron impact dissociation of N_2 and, corresponding to equation (8),

$$\frac{\mathrm{d}n_{\mathrm{NO}}}{\mathrm{d}t} = -k_1 n_{\mathrm{N}} n_{\mathrm{NO}}, \tag{25}$$

where k_1 is the rate coefficient for the reaction (R23). Thus, if only reactions (R22) and (R23) are considered in the removal of NO, the contribution from the streamer channels to the efficiency is given by expression (15) as

$$\varepsilon^{\mathrm{c}} = \frac{\left\langle I_{\mathrm{st}} \int_0^{L_{\mathrm{s}}} 2G_{\mathrm{dissoc}}(E) E\,\mathrm{d}x\right\rangle}{100 e Q n_{\mathrm{NO}}}, \tag{26}$$

where it was further considered that the concentration of NO in the background gas of N_2 is small (below 500 ppm), so that the total gas density n_0 is practically equal to the concentration of the reacting molecules n_m ($= n_{\mathrm{N_2}}$).

One could further include additional reactions such as removal of NO by the reaction

$$\mathrm{N_2^*}(a'\,^1\Sigma_{\mathrm{u}}^-) + \mathrm{NO} \rightarrow \mathrm{N_2} + \mathrm{N} + \mathrm{O}, \tag{R27}$$

in which the excited molecular nitrogen N_2^* is generated in the streamer channels by electron impact as

$$\mathrm{e} + \mathrm{N_2} \rightarrow \mathrm{e} + \mathrm{N_2^*}(a'\,^1\Sigma_{\mathrm{u}}^-), \tag{R28}$$

with rate equation

$$\frac{\mathrm{d}n_{\mathrm{N_2^*}}}{\mathrm{d}t} = k_{\mathrm{excit}} n_{\mathrm{e}} n_{\mathrm{N_2}}. \tag{29}$$

In such case the contribution of the streamer channels to the efficiency is given by expression (17) as

$$\varepsilon^{\mathrm{c}} = \frac{\left\langle I_{\mathrm{st}} \int_0^{L_{\mathrm{s}}} [2G_{\mathrm{dissoc}}(E) + G_{\mathrm{excit}}(E)]\;E\,\mathrm{d}x\right\rangle}{100 e Q n_{\mathrm{NO}}}. \tag{30}$$

To evaluate expressions (26) and (30) the G values are calculated as functions of the electric field using the Bolsig software.

The electric field was evaluated using the analytical expression of the potential of a point charge inside a cylinder at a fixed potential [18] from which one has for the potential of an azimuthally symmetric surface charge distribution $\sigma(r)$, depending on the radial cylindrical coordinate r,

$$\varphi(r,z) = \frac{1}{\pi\varepsilon_0}\int_0^{\infty}\left[\int_0^{a_{\mathrm{d}}} \sigma(r') r' I_0(kr')\,\mathrm{d}r'\right]\cos[k(z-z_d)] \times\left[K_0(kr) - I_0(kr)\frac{K_0(ka)}{I_0(ka)}\right]\mathrm{d}k, \tag{31}$$

where a is the radius of the external electrode, a_{d} is the radius of the surface charge distribution, located at the axial position z_{d}, ε_0 is the permittivity of the vacuum, and K_0 and I_0 the modified Bessel functions of order 0. Expression (31) is valid for any axial coordinate z, and for radial coordinates $a_{\mathrm{d}} \leqslant r \leqslant a$.

For a single metallic disc of radius a_{d} lying on the surface of a dielectric of relative permittivity ε_r, the total surface distribution of electric charge, including the charge on the disc plus the polarization charges on the dielectric surface, is given by [19]

$$\sigma(r) = \frac{q_{\mathrm{d}}}{2\pi\varepsilon_r a_{\mathrm{d}}^2\sqrt{1 - r^2/a_{\mathrm{d}}^2}}, \tag{32}$$

where q_d is the electric charge in the disc only. Use of the expression (32) in (31) results in the analytical expression for the potential due to a disc on a dielectric surface as

$$\varphi(r,z) = \frac{q_d}{2\pi^2\varepsilon_r\varepsilon_0}\int_0^\infty \cos\left[k(z-z_d)\right]\frac{\sinh(ka_d)}{ka_d} \times\left[K_0(kr) - I_0(kr)\frac{K_0(ka)}{I_0(ka)}\right]\mathrm{d}k, \quad (33)$$

in which the k integral is to be done numerically. The actual potential distribution is determined as the superposition of an expression (33) for each disc. This expression, when evaluated at each disc position, allows to relate the disc charges with the disc voltages (which are the actual inputs), and the electric field is finally obtained by numerical spatial derivation.

To evaluate the spatial integrals at each measured instant in expressions (26) and (30) we have considered the radial electric field in the plane of the active electrode disc, in the region between the disc border and the external electrode. This evaluation was done for each measured instantaneous value of the disc voltage, during an integer number of time periods of this periodic voltage. The value of this integral is then multiplied by the corresponding instantaneous streamer current, I_{st}, and the time average evaluated as the arithmetic average of all these products.

For the contribution of the steamer heads the expression corresponding to equation (30) is, from equation (21),

$$\varepsilon^h = \frac{\langle I_{st}\rangle\int_{r_h}^\infty\left[2G_{dissoc}(E_h)+G_{excit}(E_h)\right]E_h\,\mathrm{d}r}{100eQn_{NO}}, \quad (34)$$

where E_h is given by expression (19).

5. Results and discussions

Typical signals of the voltage V_{ac}, the DBD current (I_{DBD}), and the interelectrode current (I) for V_{ac} peak-to-peak value $V_{ac}^p = 11\,\mathrm{kV}$ and $V_{dc} = -12\,\mathrm{kV}$ are shown in figure 2. The presence of streamers crossing the electrode gap is appreciated as a series of pulses superposed on the capacitive current.

The time evolution of the NO concentration is shown in figure 3 for different values of $V_{ac}^p$and V_{dc}. Cases a) and b) correspond to $V_{dc} = -10\,\mathrm{kV}$, with $V_{ac}^p = 10\,\mathrm{kV}$ and 11 kV, respectively and cases (c), (d) and (e) correspond to a $V_{dc} = -12\,\mathrm{kV}$, with $V_{ac}^p = 9\,\mathrm{kV}$, 10 kV and 11 kV, respectively. For all cases, the initial NO concentration (NO_i) was about 490 ppm, and after the discharge ignition, the NO concentration reached a constant value (NO_f). It can be seen from figure 3 that when the voltage difference applied across the electrode gap (V_{ac}–V_{dc}) increases, the final concentration of NO decreases. The lowest final concentration achieved was 270 ppm for $V_{ac}^p = 11\,\mathrm{kV}$ and $V_{dc} = -12\,\mathrm{kV}$. It is worth noting that the characteristic time of NO concentration decay, apparent in figure 3, is associated to the delay in the arrival of the treated portion of the gas to the gas analyser, and not to any reaction time. In fact, the theoretical model assumes that the reactions are instantaneous compared to the permanence time of the gas in the reactor.

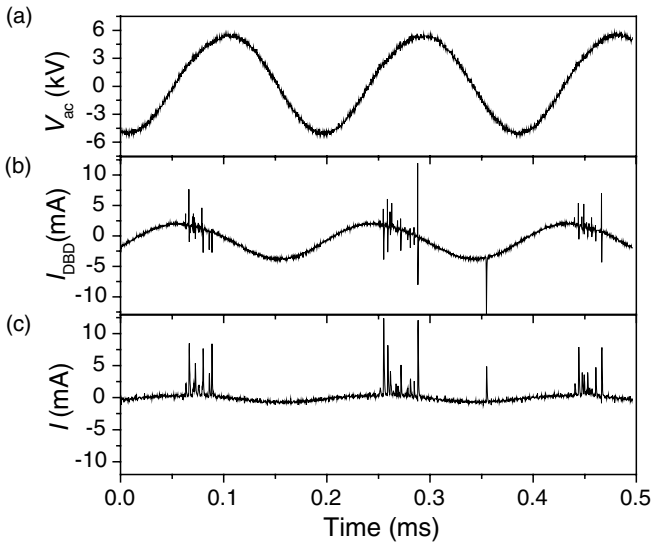

Figure 2. Typical signals of the voltage V_{ac} (a), DBD current (b), and interelectrode current (c).

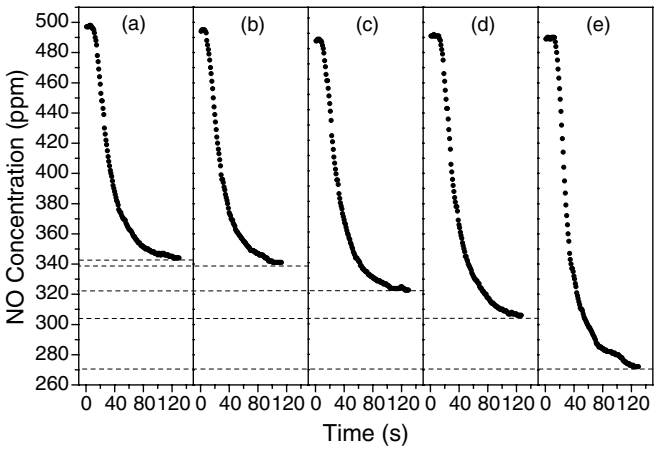

Figure 3. NO concentration as function of time for different electrode potential. (a) $V_{dc} = -10\,\mathrm{kV}$, $V_{ac}^p = 10\,\mathrm{kV}$, ($b$) $V_{dc} = -10\,\mathrm{kV}$, $V_{ac}^p = 11\,\mathrm{kV}$, ($c$) $V_{dc} = -12\,\mathrm{kV}$, $V_{ac}^p = 9\,\mathrm{kV}$, ($d$) $V_{dc} = -12\,\mathrm{kV}$, $V_{ac}^p = 10\,\mathrm{kV}$, ($e$) $V_{dc} = -12\,\mathrm{kV}$, $V_{ac}^p = 11\,\mathrm{kV}$.

The experimental removal efficiency ($\varepsilon_{exp}\%$) was calculated as:

$$\varepsilon_{exp}\% = \frac{\langle NO_i - NO_f\rangle}{NO_i}\times 100.$$

Also, the theoretical evaluation of the efficiency, equation (30), was done using the inputs of two time periods of V_{ac} and The I streamer current was determined by simply taking the current values above the maximum of the capacitive current, and subtracting this last value. The G values as functions of reduced electric field were obtained using the Bolsig software. In figure 4 the G values for dissociation and excitation of N_2 are shown. It can be seen that there is a strong dependence of G on the reduced field for the values below 100 Td. The reduced electric field in the streamer channel of the discharge for all the cases studied is below 120 Td, using the air number density corresponding to normal conditions $N = 2.45\times10^{25}\,\mathrm{m}^{-3}$.

Concerning the evaluation of the streamer heads contribution to the efficiency, we have first verified that,

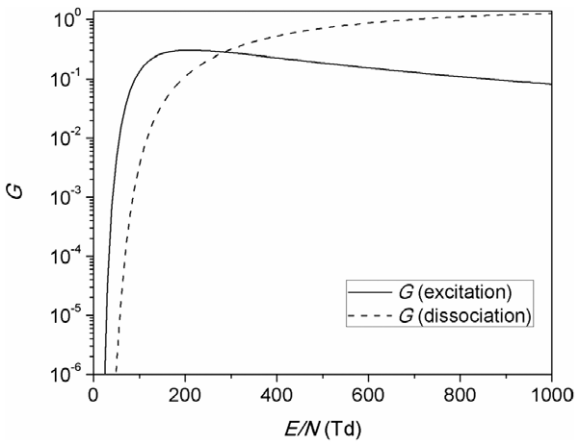

Figure 4. G-values for dissociation and excitation of N_2 molecules by electron impact, as functions of the reduced electric field in Townsend units (Td), used in the theoretical evaluation of the efficiency.

rewriting equation (34) as,

$$\int_{r_h}^{\infty} [2G_{\text{dissoc}}(E_h) + G_{\text{excit}}(E_h)]\, E_h\, \mathrm{d}r = \varepsilon^h \frac{\langle I_{st}\rangle}{100 e Q n_{NO}} \tag{35}$$

and evaluating ε^h as the difference between the measured total efficiency and the calculated streamer channel efficiency,

$$\varepsilon^h = \varepsilon_{exp} - \varepsilon^c$$

similar values of the right-hand side in (35) were obtained for all cases studied, as it should if the assumption of similar electric field distributions of the streamer heads is valid. The average value obtained was $1.23 \times 10^4 C^{-1}$, with all values differing in at most 13%. In this way, the streamer heads contribution to the efficiency was evaluated using expression (34) with this average value for the integral.

Note that the integral depends on two parameters, r_h and $E_{h\,max}$. In this way, for each possible r_h there is a corresponding $E_{h\,max}$ that fits the obtained average value of the integral. For instance, for $r_h = 5 \times 10^{-4}$m the corresponding reduced maximum field is 10^3 Td, while to $r_h = 10^{-3}$m corresponds 700 Td, which are reasonable values, within the range of reported magnitudes [12, 20–23].

On the other hand, for the evaluation of the separate contribution of each reaction (dissociation and excitation) to the efficiency we must use particular values of r_h and $E_{h\,max}$. In our case, we have chosen for reference $E_{h\,max}$ corresponding to a reduced field of 700 Td and corresponding $r_h = 10^{-3}$ m.

In table 1 the experimental and theoretical efficiencies for all cases studied are presented. Moreover, the contribution to the theoretical efficiency through reaction (R23) by the atomic N generated by the dissociation reaction (R22) (ε_{diss}), and by the atomic N resulting from reaction (R27) (ε_{exc}) are presented separately, and also separated by the contributions from the channels and heads. As can be appreciated, the total theoretical efficiency follows the same trend of the experimental one and both agree reasonable well.

An important point is that the relative contributions from the dissociation and excitation reactions to the theoretical efficiency vary in the different cases. This is due to the highly non-linear dependence of the G values on the electric field, apparent in figure 4. Moreover, in all cases, the streamer head contribution to the efficiency related to the dissociation is greater than that related to the excitation, due to the large values of the reduced field in the streamer heads and the corresponding larger G values for dissociation in this region, as shown in figure 4.

From the electrical signal, the average power (P) input to the discharge was calculated as:

$$P = \frac{\left\langle \int_0^T [(V_{ac} - V_{dc})I + V_{ac} I_{DBD}]\ \mathrm{d}t \right\rangle}{T}$$

where T is the period of the V_{ac} signal and I_{DBD} is the current across the discs. For a technological application it is important to evaluate the energy cost per removed NO molecule (E_c). The parameter E_c in (eV/molecule) was calculated using the following formula [24, 25]

$$E_c\left[\text{eV/molecule}_{NO}\right] = \left[P\,[\text{W}]\ \ 6.25 \times 10^{18}\left[\text{eV J}^{-1}\right]\right] \times \left[Q\left[1\,\text{min}^{-1}\right]\frac{1}{60}\left[\text{min s}^{-1}\right]\varepsilon_{exp}\%\text{NO}_i\,[\text{ppm}]\,10^{-8}\ \ 2.45 \times 10^{22}\left[\text{molecules l}^{-1}\right]\right].$$

Another widely used parameter is the energy yield E_Y in (mol/kWh) which was calculated as the reciprocal of the energy cost multiplied by a factor for conversion of units [26]. In table 2 the power input to the discharge, the energy cost and the energy yield for all the cases studied are presented.

Note that for fixed V_{dc} the energy cost E_c decreases (and E_y increases) as V_{ac}^p increases, indicating a more efficient production of streamers by a more intense DBD. For $V_{dc} = -12$ kV the values of E_y are close to those in pulsed CDs, while the E_y for $V_{dc} = -10$ kV are similar to those obtained in nano-second pulsed discharges [26], indicating a good performance of the reactor for NO removal comparable to those energetically most efficient discharge methods.

6. Conclusions

We have presented an experimental and theoretical study of a three-electrode discharge configuration for the removal of NO. This particular reactor has a region of low impedance to the gas flow, with long streamers permeating its cross section. Experimentally, it is found that the discharge configuration can be as efficient energetically as reactors employing nano-second discharge methods, probably because the reactive species generated in the streamer are effectively entrained in the flow, due to the mentioned good pervasion of the streamers into the gas region. The increase of the energy yield E_y as the DBD voltage increases indicates also a possible way to further optimize the energetic performance of the reactor. From the theoretical side, the model allows to quantify the contribution of the different processes to the pollutant removal efficiency, and has the advantage of reducing the inputs needed to only the bias voltages and electric current of the discharge, together

Table 1. Experimental and theoretical efficiencies for different applied voltages. Theoretical values are given as streamer head + channel contributions.

Case	$\varepsilon_{exp\%}$	$\varepsilon_{theo\%}$	$\varepsilon_{diss\%}$	$\varepsilon_{exc\%}$
a ($V_{dc} = -10$ kV, $V_{ac}^{p} = 10$ kV)	30	25.7 + 1.0	20.4 + 0.5	5.3 + 0.5
b ($V_{dc} = -10$ kV, $V_{ac}^{p} = 11$ kV)	30	27.2 + 1.0	21.5 + 0.5	5.7 + 0.5
c ($V_{dc} = -12$ kV, $V_{ac}^{p} = 9$ kV)	34	33.3 + 1.5	26.3 + 0.5	7.0 + 1.0
d ($V_{dc} = -12$ kV, $V_{ac}^{p} = 10$ kV)	38	40.8 + 2.5	32.3 + 1.0	8.5 + 1.5
e ($V_{dc} = -12$ kV, $V_{ac}^{p} = 11$ kV)	45	43.8 + 3.0	34.6 + 1.0	9.2 + 2.0

Table 2. Power input to the discharge, energy cost and energy yield for different applied voltage. The power input indicated between brackets corresponds to that associated to the streamers crossing the interelectrode gas, plus that associated to the DBD, respectively.

Case	P (W)	E_c (eV/molecule$_{NO}$)	E_y (mol kWh^{-1})
a ($V_{dc} = -10$ kV, $V_{ac}^{p} = 10$ kV)	1.33 (1.04 + 0.29)	69.2	0.54
b ($V_{dc} = -10$ kV, $V_{ac}^{p} = 11$ kV)	1.49 (1.19 + 0.30)	63.3	0.59
c ($V_{dc} = -12$ kV, $V_{ac}^{p} = 9$ kV)	1.94 (1.64 + 0.30)	111.5	0.33
d ($V_{dc} = -12$ kV, $V_{ac}^{p} = 10$ kV)	2.54 (2.24 + 0.30)	104.2	0.36
e ($V_{dc} = -12$ kV, $V_{ac}^{p} = 11$ kV)	2.65 (2.33 + 0.32)	89.1	0.42

with a simple parameterization of the streamer head. In case that these inputs can be assumed as given, independently of the pollutant type and concentration, the model can be used in a predictive way to evaluate the efficiency of the given reactor for the removal of different pollutants. Also, it was verified, in agreement with recent studies [12, 15], that the streamer heads contribute to most of the production of reactive species generated by electron impact in these particularly high energy-threshold reactions.

In this work we considered only the case of NO reduction by N radicals. In other gas mixtures other reactions should be included, for example, in air, the generation of atomic O by dissociation of O_2 by electron impact, and by the reaction of O_2 with N_2 excited by electron impact, as the main ones [12]. The contribution to the removal efficiency of reactions involving NO with the generated O can be taken into account using the general formulas (17) and (21). In particular, as the G-values of the processes just mentioned are relatively high at lower values of the reduced field, as compared with those related to N, the contribution of the streamers channels is expected to be significant.

Acknowledgments

The authors are glad to acknowledge grants from the Agencia Nacional de Promoción Científica y Tecnológica (ANPCyT), grant PICT 2010-0771, the Consejo Nacional de Investigaciones Científicas y Técnicas (CONICET), grant PIP 11220090100219. JLG and the University of Buenos Aires (UBA), grant UBACYT 20020090100141 also acknowledges a doctoral fellowship awarded by CONICET.

References

[1] Masuda S and Nakao H 1990 Control of NO_x by positive and negative pulsed corona discharges *IEEE Trans. Industry Appl.* **26** 374–383

[2] Shang K, Zhuo Y and Wu Y 2009 Simultaneous removal of SO_2/NO_x by corona discharge plasma *ICEET '09 Int. Conf. on Energy and Environment Technology (Guilin)* vol 3 pp 106–9

[3] Mizuno A 2007 Industrial applications of atmospheric non-thermal plasma in environmental remediation *Plasma Phys. Control. Fusion* **49** A1–15

[4] Khacef A and Cormier J M 2006 Pulsed sub-microsecond dielectric barrier discharge treatment of simulated glass manufacturing industry flue gas: removal of SO_2 and NO_x *J. Phys. D: Appl. Phys.* **39** 1078–83

[5] Wang T, Sun B-M, Xiao H-P, Zeng J-Y, Duan E-P, Xin J and Li C 2012 Effect of Reactor Structure in DBD for nonthermal plasma processing of NO in N_2 at ambient temperature *Plasma Chem. Plasma Process.* **32** 1189–201

[6] Pacheco M, Alva E, Valdivia R, Pacheco J, Rivera C, Santana A, Huertas J, Lefort B and Estrada N 2012 Removal of main exhaust gases of vehicles by a double dielectric barrier discharge *J. Phys.: Conf. Ser.* **370** 012023

[7] Van Durme J, Dewulf J, Ley C and Van Langenhove H 2008 Combining non-thermal plasma with heterogeneous catalysis in waste gas treatment: a review *Appl. Catal.* B **78** 324–33

[8] Dors M, Mizeraczyk J, Nichipor G V and Mok Y S 2005 The role of surface reactions in de-NO_x processes in corona discharge-catalyst (or zeolite) hybrid systems *J. Adv. Oxid. Technol.* **8** 212–17

[9] Yu Q, Wang H, Liu T, Xiao L, Jiang X and Zheng X 2012 High-efficiency removal of NO_x using a combined adsorption-discharge plasma catalytic process *Environ. Sci. Technol.* **46** 2337–44

[10] Grondona D, Allen P and Kelly H 2011 Development of a coaxial-stacked trielectrode plasma curtain *IEEE Trans. Plasma Sci.* **39** 1466–9

[11] Penetrante B M, Hsiao M C, Merritt B T, Vogtlin G E, Wallman P H, Neiger M, Wolf O, Hammer T and Broer S 1996 Pulsed corona and dielectric-barrier discharge processing of NO in N_2 *Appl. Phys. Lett.* **68** 3719–21

[12] Naidis G V 2012 Efficiency of generation of chemically active species by pulsed corona discharges *Plasma Sources Sci. Technol.* **21** 042001

[13] Penetrante B M, Hsiao M C, Merritt B T, Vogtlin G E and Wallman P H 1995 Comparison of electrical discharge techniques for nonthermal plasma processing of NO in N_2 *IEEE Trans. Plasma Sci.* **23** 679–87

[14] Hagelaar G J M and Pitchford L C 2005 Solving the Boltzmann equation to obtain electron transport coefficients and rate coefficients for fluid models *Plasma Sources Sci. Technol.* **14** 722–33
[15] Kozlov V K, Wagner H-E, Brandenburg R and Michel P 2001 Spatio-temporal resolved spectroscopic diagnostics of the barrier discharge in air at atmospheric pressure *J. Phys. D: Appl. Phys.* **34** 3164–76
[16] Sato N 1980 Discharge current induced by the motion of charged particles *J. Phys. D: Appl. Phys.* **13** L3–6
[17] Aleksandrov N L and Bazelyan E M 1996 Simulation of long-streamer propagation in air at atmospheric pressure *J. Phys. D: Appl. Phys.* **29** 740–52
[18] Hernandes J A and Assis A K T 2005 Electric potential due to an infinite conducting cylinder with internal or external point charge *Electrostat J.* **63** 1115–31
[19] Liang C H, Li L and Zhi H Q 2004 Asymptotic closed form for the capacitance of an arbitrarily shaped conducting plate *IEEE Proc. Microw. Antennas* **151** 217–20
[20] Briels T M P, Kos J, Winands G J J, van Veldhuizen E M and Ebert U 2008 Positive and negative streamers in ambient air: measuring diameter, velocity and dissipated energy *J. Phys. D: Appl. Phys.* **41** 234004
[21] Lago V, Grondona D, Kelly H, Sosa R, Márquez A and Artana G 2009 Sliding Discharge Optical Emission Characteristics *IEEE Trans. Electr. Insul.* **16** 292–8
[22] Bazelyan E M and Raizer Yu P 1998 *Spark Discharge* (Boca Raton, FL: CRC Press)
[23] Starikovskaia S M, Allegraud K, Guaitella O and Rousseau A 2010 On electric field measurements in surface dielectric barrier discharge *J. Phys. D: App. Phys.* **43** 124007
[24] Mohapatro S, Rajanikanth B S, Rajkumar R B, Ramadas C and Mishra A 2011 Treatment of NO_x from diesel engine exhaust by dielectric barrier discharge method *ACEEE Int. J. Commun.* **2** 1–4
[25] Kim H H 2004 Nonthermal plasma processing for air-pollution control: a historical review, current issues, and future prospects *Plasma Process. Polym.* **1** 91–110
[26] Matsumoto T, Wang D, Namihira T and Akiyama H 2010 Energy efficiency improvement of nitric oxide treatment using nanosecond pulsed discharge *IEEE Trans. Plasma Sci.* **38** 2639–43